Robust SINS/GNSS Integration Method for High Dynamic Applications

Falin Wu[1], Hengyang Zhao[1]*, Yan Zhao[1], Haibo Zhong[2]
[1]School of Instrumentation Science and Opto-electronics Engineering, Beihang University,
Beijing 100191, China
[2]Space Star Technology Co. Ltd, Beijing, 100086, China
*Corresponding author, e-mail: hengyang178@163.com

Abstract

As high dynamic movement is always accompanied by colored noise which lacks of mathematical model, traditional Kalman filtering based on an assumption of white Gaussian noise always faces serious divergence. To enhance the performance in high dynamic environment with uncertain colored noise, a kind of robust filtering based on H-infinity technology is developed. State model of the algorithm is derived from SINS error propagation. Both position and velocity errors are used as the measurements. A simulation system which includes a tri-axial turntable and a GNSS signal simulator is used to verify the integration design under high dynamic environment. Simulation results proved that both the accuracy and robustness of the integration design have been improved significantly.

Keywords: SINS/GNSS integration, high dynamic, H-infinity Kalman filtering

1. Introduction

Strapdown Inertial Navigation System (SINS) is a kind of dead reckoning method based on Inertial Measurement Unit (IMU) [1]. As the navigation error will get accumulated, the precision of IMU determines the navigation effect mainly. Global Navigation Satellite System (GNSS) is a kind of high precision positioning solution which could provide position and velocity information by a single receiver [2]. But the usage of GNSS is limited because of the signal attenuation in urban canyon or situation with strong electromagnetic interference. Furthermore, the low output rate of GNSS limits its usage in high dynamic environment. SINS/GNSS integration mixes their advantages and disadvantages respectively where the Kalman filtering (KF) is commonly used [3, 4].

High dynamic movement is always accompanied with uncertain colored noise [5]. However, traditional Kalman filter relies on the assumption that both process noise and measurement noise are uncorrelated white Gaussian noise which will result in the divergent of navigation results. Technologies such as robust filtering has been developed to enhance navigation performance under high dynamic environment [6, 7]. H-infinity filtering is a kind of robust filtering technology which could retard filtering divergence effectively in colored noise environment [8]. There is no requirement of noise priori knowledge but just having finite bounded energies. H-infinity filtering based on traditional Kalman filtering does not destroy the linearity and only need the transformation of the covariance matrix calculation.

In this paper, a kind of H-infinity Kalman filter algorithm for SINS/GNSS integrated navigation system is designed. The process model is based on SINS error propagation. Errors of both position and velocity are used as measurements. H-infinity filtering was used to enhance system robustness. At last, a comparison of H-infinity Kalman filtering with the traditional Kalman filtering has been drawn using a hardware-in-the–loop simulation system.

2. Integration Design

Structure of the integration design is shown in Figure 1.
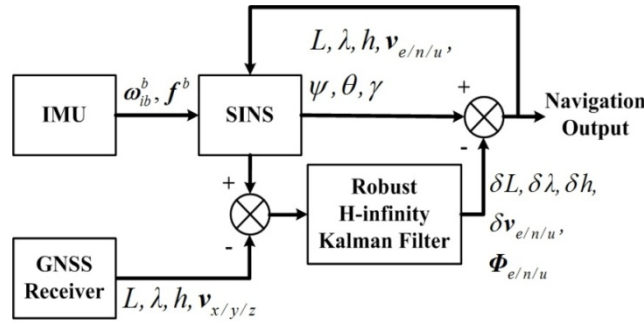
Figure 1. Integration structure

SINS algorithm is applied based on gyroscope angular velocity ω_{ib}^b and accelerometer specific force f^b which acquired from IMU. Errors between SINS and GNSS receiver outputs are used as measurements of the filter. Filter estimation outputs will modify the SINS outputs which used as the final outputs and feedback to the next SINS iteration at the same time. Beside these, L, λ and h are latitude, longitude and altitude with δL, $\delta \lambda$ and δh as the errors. $v_{e/n/u}$ are velocities in geographic coordinate (i.e., east, north and up) with $\delta v_{e/n/u}$ as the errors. ψ, θ and γ are craft attitude (i.e., yaw, pitch and roll) from t frame (True frame or navigation frame) coordinate to b frame (Body frame or craft frame) coordinate. $\Phi_{e/n/u}$ are misalignment angles from t frame to c frame (Computer frame) coordinate [9]. $v_{x/y/z}$ are velocities in earth fixed coordinate as parts of GNSS receiver outputs.

2.1. Process Model
Process model of the SINS/GNSS integration is:

$$\dot{X} = FX + GW \tag{1}$$

where X is the estimation state variable with covariance matrix P.

$$
\begin{cases}
X = \begin{bmatrix} \Phi_e & \Phi_n & \Phi_u & \delta v_e & \delta v_n & \delta v_u & \delta L & \delta \lambda & \delta h & \varepsilon_x & \varepsilon_y & \varepsilon_z & \nabla_x & \nabla_y & \nabla_z \end{bmatrix}^T \\
P = \mathrm{diag}\left(\sigma_{\Phi_e}^2, \ \sigma_{\Phi_n}^2, \ \sigma_{\Phi_u}^2, \ \sigma_{\delta v_e}^2, \ \sigma_{\delta v_n}^2, \ \sigma_{\delta v_u}^2, \ \sigma_{\delta L}^2, \ \sigma_{\delta \lambda}^2, \ \sigma_{\delta h}^2, \ \sigma_{\varepsilon_x}^2, \ \sigma_{\varepsilon_y}^2, \ \sigma_{\varepsilon_z}^2, \ \sigma_{\nabla_x}^2, \ \sigma_{\nabla_y}^2, \ \sigma_{\nabla_z}^2 \right)
\end{cases} \tag{2}
$$

Where $\sigma_{\Phi_{e/n/u}}^2$, $\sigma_{\delta v_{e/n/u}}^2$ and $\sigma_{\delta L/\lambda/h}^2$ are variance of misalignment angles, velocity errors and position errors. $\varepsilon_{x/y/z}$ and $\nabla_{x/y/z}$ are gyroscope drift and accelerometer bias at b frame coordinate with variance $\sigma_{\varepsilon_{x/y/z}}^2$ and $\sigma_{\nabla_{x/y/z}}^2$.

W is additive zero mean white Gaussian noise of the IMU with covariance matrix Q.

$$
\begin{cases}
W = \begin{bmatrix} \omega_{gx} & \omega_{gy} & \omega_{gz} & \omega_{ax} & \omega_{ay} & \omega_{az} \end{bmatrix}^T \\
Q = \mathrm{diag}\left(\sigma_{gx}^2, \ \sigma_{gy}^2, \ \sigma_{gz}^2, \ \sigma_{ax}^2, \ \sigma_{ay}^2, \ \sigma_{az}^2 \right)
\end{cases} \tag{3}
$$

Where $\omega_{gx/gy/gz}$ and $\omega_{ax/ay/az}$ are gyroscope and accelerometer noise process with variance $\sigma_{gx/gy/gz}^2$ and $\sigma_{ax/ay/az}^2$.

Process noise input matrix G is given as:

$$
G = \begin{bmatrix} 0_{3\times3} & 0_{3\times3} & 0_{3\times3} & 0_{3\times3} & I_{3\times3} \\ 0_{3\times3} & 0_{3\times3} & 0_{3\times3} & I_{3\times3} & 0_{3\times3} \end{bmatrix}^T \tag{4}
$$

State transition matrix $\boldsymbol{F}$ could be extracted from propagation of misalignment angles, velocity errors, position errors and IMU errors which can be expressed as below [10].

$$
\begin{cases}
\dot{\phi_e} = (\omega_{ie}\sin L + \dfrac{v_e}{R_n+h}\tan L)\phi_n - (\omega_{ie}\cos L + \dfrac{v_e}{R_n+h})\phi_u - \dfrac{\delta v_n}{R_m+h} + \varepsilon_e \\[2ex]
\dot{\phi_e} = -(\omega_{ie}\sin L + \dfrac{v_e}{R_n+h}\tan L)\phi_e - \dfrac{v_n}{R_m+h}\phi_u + \dfrac{\delta v_e}{R_n+h} - \omega_{ie}\sin L\,\delta L + \varepsilon_n \\[2ex]
\dot{\phi_u} = (\omega_{ie}\cos L + \dfrac{v_e}{R_n+h})\phi_e + \dfrac{v_n}{R_m+h}\phi_n + \dfrac{\delta v_e}{R_n+h}\tan L + (\omega_{ie}\cos L + \dfrac{v_e}{R_n+h}\sec^2 L)\delta L + \varepsilon_u
\end{cases}
\tag{5}
$$

$$
\begin{cases}
\delta\dot{v_e} = f_n\phi_u - f_u\phi_n + (\dfrac{v_n}{R_m+h}\tan L - \dfrac{v_u}{R_m+h})\delta v_e \\[2ex]
\qquad + (2\omega_{ie}\sin L + \dfrac{v_e}{R_n+h}\tan L)\delta v_n - (2\omega_{ie}\cos L + \dfrac{v_e}{R_n+h})\delta v_u \\[2ex]
\qquad + (2\omega_{ie}\cos L v_n + \dfrac{v_e v_n}{R_n+h}\sec^2 L + 2\omega_{ie}\sin L v_u)\delta L - \dfrac{v_e v_u - v_e v_n \tan L}{(R_n+h)^2}\delta h + \nabla_e \\[2ex]
\delta\dot{v_n} = f_u\phi_e - f_e\phi_u - 2(\omega_{ie}\sin L + \dfrac{v_e}{R_n+h}\tan L)\delta v_e - \dfrac{v_u}{R_m+h}\delta v_n - \dfrac{v_n}{R_m+h}\delta v_u \\[2ex]
\qquad - (2\omega_{ie}\cos L + \dfrac{v_e}{R_n+h}\sec^2 L)v_e\delta L + \dfrac{v_e v_u + v_e^2 \tan L}{(R_m+h)(R_n+h)}\delta h + \nabla_n \\[2ex]
\delta\dot{v_u} = f_e\phi_n - f_n\phi_e - 2(\omega_{ie}\cos L + \dfrac{v_e}{R_n+h})\delta v_e + \dfrac{2v_n}{R_m+h}\delta v_u \\[2ex]
\qquad - 2\omega_{ie}\sin L v_e\delta L + 2\omega_{ie}\sin L v_e\delta h + \nabla_u
\end{cases}
\tag{6}
$$

$$
\begin{cases}
\delta\dot{L} = \dfrac{\delta v_n}{R_m+h} - \dfrac{v_n}{(R_m+h)(R_n+h)}\delta h \\[2ex]
\delta\dot{\lambda} = \dfrac{\delta v_e}{R_n+h}\sec L + \dfrac{v_e}{R_n+h}\sec L\tan L\,\delta L - \dfrac{v_e}{(R_m+h)(R_n+h)}\delta h \\[2ex]
\delta\dot{h} = \delta v_u
\end{cases}
\tag{7}
$$

$$
\begin{cases}
\dot{\varepsilon}_{x/y/z} = \omega_{gx/gy/gz} \\[1ex]
\dot{\nabla}_{x/y/z} = \omega_{ax/ay/az}
\end{cases}
\tag{8}
$$

Where $f_{e/n/u}$, $\varepsilon_{e/n/u}$ and $\nabla_{e/n/u}$ denote the specific force, gyroscope drift and accelerometer bias at t frame, respectively. ω_{ie} is the rotational angular velocity of the earth. R_m and R_n used above are radius of meridian plane and prime vertical plane which can be calculated as:

$$
\begin{cases}
R_m = \dfrac{R_e}{1+2e-3e\sin(L^2)} \\[2ex]
R_n = \dfrac{R_e}{1-e\sin(L^2)}
\end{cases}
\tag{9}
$$

Where R_e represents the radius of the earth and e is the earth eccentrity.

2.2. Measurement Model

Measurement model is based on position error and velocity error at geographical coordinate which can be expressed as:

$$Z = HX + V \tag{10}$$

Where Z is the measurement given as:

$$Z = \begin{bmatrix} \delta v_e & \delta v_n & \delta v_u & \delta L & \delta \lambda & \delta h \end{bmatrix}^T$$
$$= \begin{bmatrix} v_{e,SINS} - v_{e,GNSS} & v_{n,SINS} - v_{n,GNSS} & v_{u,SINS} - v_{u,GNSS} & L_{SINS} - L_{GNSS} & \lambda_{SINS} - \lambda_{GNSS} & h_{SINS} - h_{GNSS} \end{bmatrix}^T \tag{11}$$

The GNSS receiver has velocity outputs at earth ECEF (Earth Centered Earth Fixed) coordinate as $v_{x/y/z,GNSS}$ which have to be transferred into geographical coordinate as $v_{e/n/u,GNSS}$.

$$\begin{bmatrix} v_{e,GNSS} \\ v_{n,GNSS} \\ v_{u,GNSS} \end{bmatrix} = \begin{bmatrix} \cos\left(\dfrac{\pi}{2}+\lambda\right) & \sin\left(\dfrac{\pi}{2}+\lambda\right) & 0 \\ -\cos\left(\dfrac{\pi}{2}-L\right)\sin\left(\dfrac{\pi}{2}+\lambda\right) & \cos\left(\dfrac{\pi}{2}-L\right)\cos\left(\dfrac{\pi}{2}+\lambda\right) & \sin\left(\dfrac{\pi}{2}-L\right) \\ \sin\left(\dfrac{\pi}{2}-L\right)\sin\left(\dfrac{\pi}{2}+\lambda\right) & -\sin\left(\dfrac{\pi}{2}-L\right)\cos\left(\dfrac{\pi}{2}+\lambda\right) & \cos\left(\dfrac{\pi}{2}-L\right) \end{bmatrix} \begin{bmatrix} v_{x,GNSS} \\ v_{y,GNSS} \\ v_{z,GNSS} \end{bmatrix} \tag{12}$$

The measurement matrix is given as:

$$H = \begin{bmatrix} \mathbf{0}_{3\times3} & \mathbf{I}_{3\times3} & \mathbf{0}_{3\times3} & \mathbf{0}_{3\times3} & \mathbf{0}_{3\times3} \\ \mathbf{0}_{3\times3} & \mathbf{0}_{3\times3} & \mathbf{I}_{3\times3} & \mathbf{0}_{3\times3} & \mathbf{0}_{3\times3} \end{bmatrix} \tag{13}$$

V is zero mean white Gaussian noise with covariance matrix R.

$$\begin{cases} V = \begin{bmatrix} v_{v_e} & v_{v_n} & v_{v_u} & v_L & v_\lambda & v_h \end{bmatrix}^T = \begin{bmatrix} v_{v_h} & v_{v_h} & v_{v_v} & v_{p_h}/R_e & v_{p_h}/R_e & v_{p_v} \end{bmatrix}^T \\ R = \mathrm{diag}\left(\sigma_{v_e}^2,\ \sigma_{v_n}^2,\ \sigma_{v_u}^2,\ \sigma_L^2,\ \sigma_\lambda^2,\ \sigma_h^2\right) = \mathrm{diag}\left(\sigma_{v_h}^2,\ \sigma_{v_h}^2,\ \sigma_{v_v}^2,\ \left(\sigma_{p_h}/R_e\right)^2,\ \left(\sigma_{p_h}/R_e\right)^2,\ \sigma_{p_v}^2\right) \end{cases} \tag{14}$$

Where $v_{v_{e/n/u}}$ are GNSS velocity measurement noises at geographical coordinate which can also be expressed as horizontal and vertical noise v_{v_h} and v_{v_v} with variances of $\sigma_{v_h}^2$ and $\sigma_{v_v}^2$. $v_{L/\lambda/h}$ are GNSS geographical position measurement noises transferred from horizontal and vertical noise v_{p_h} and v_{p_v} with variances of $\sigma_{p_h}^2$ and $\sigma_{p_v}^2$.

2.3. H-infinity Kalman Filter

Discretization of the process model and measurement model is represented as:

$$\begin{cases} X_{k+1} = \Phi_{k+1/k} X_k + \Gamma_k W_k \\ Z_k = H_k X_k + V_k \end{cases} \tag{15}$$

Assume T_{KF} is the calculation period of the Kalman filter. Φ and Γ are given as:

$$\begin{cases} \Phi = I + F T_{KF} \\ \Gamma = G T_{KF} + F\, T_{KF}^2 / 2 \end{cases} \tag{16}$$

Assume $\hat{X}_k$ is the state estimation with variance P_k, the recursion algorithm of the H-infinity filtering can be expressed as:

$$
\begin{cases}
R_{e,k+1} = \begin{bmatrix} R & 0 \\ 0 & -\gamma^2 I \end{bmatrix} + \begin{bmatrix} H_k \\ L_k \end{bmatrix} P_k \begin{bmatrix} H_k^T & L_k^T \end{bmatrix} \\
P_{k+1} = \Phi_{k+1/k} P_k \Phi_{k+1/k}^T + \Gamma_k Q \Gamma_k^T - \Phi_{k+1/k} P_k \begin{bmatrix} H_k^T & L_k^T \end{bmatrix} R_{e,k}^{-1} \begin{bmatrix} H_k \\ L_k \end{bmatrix} P_k \Phi_{k+1/k}^T \\
K_{k+1} = P_{k+1} H_{k+1}^T \left(H_{k+1} P_{k+1} H_{k+1}^T + R \right)^{-1} \\
\hat{X}_{k+1} = \Phi_{k+1/k} \hat{X}_k + K_{k+1} \left(Z_{k+1} - H_{k+1} \Phi_{k+1/k} \hat{X}_k \right)
\end{cases}
\tag{17}
$$

Where $L_k = I$ and $\gamma^2 = \alpha \max \left(\mathrm{eig} \left(P_k^{-1} + H_k^T H_k \right)^{-1} \right)$. $\max \left(\mathrm{eig}(M) \right)$ means the maximum eigenvalue of matrix M. $\alpha > 1$ is a parameter used to guarantee the positiveness of P_k and control the tradeoff between robustness and precision [11]. The value of α is set as 10 in this system.

4. Validation and Analysis

To verify the integration design, a hardware-in-the-loop simulation system has been developed [12]. The system includes a IMU, a GNSS receiver, a trajectory simulator, a tri-axial turntable, a GNSS signal simulator and a navigation computer as shown in Figure 2.
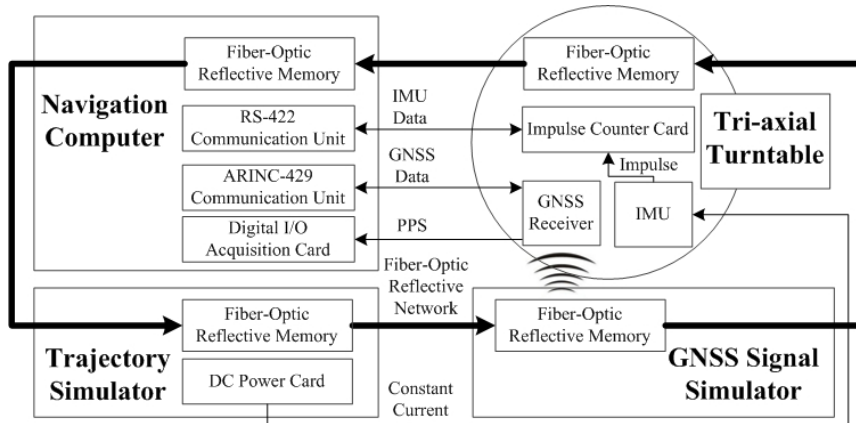
Figure 2. Simulation system structure
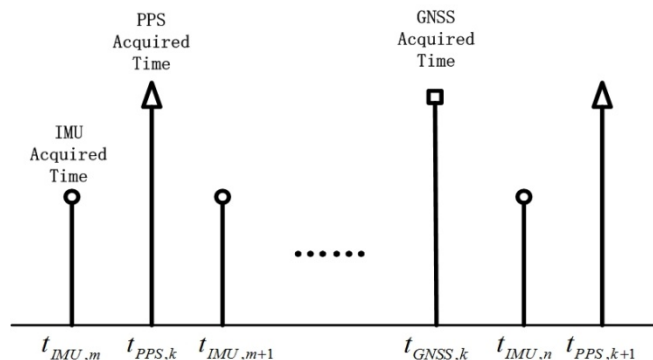
Figure 3. Time synchronization diagram

The system is built on annular fiber-optic communication network to ensure instantaneity [13]. The IMU contains a tri-axial fiber-optic gyroscope and a tri-axial pendulous integrating accelerometer with output frequency of 100Hz. The GNSS receiver outputs navigation data and PPS (Pulses Per Second) [14] at frequency of 10Hz. The accelerometer outputs desired acceleration under external current injection which comes form three electric isolated channels on the DC power board [15]. Impulse counter board is used to receive and transform continuous impulses come from the IMU [16]. The navigation computer is used to receive and synchronize data as shown in Figure 3 and implement the integration algorithm.

The basic SINS algorithm will be done firstly when the IMU data has been acquired. Assume the SINS has output of $x_{SINS}(t_{IMU,m})$ and $x_{SINS}(t_{IMU,m+1})$ at time $t_{IMU,m}$ and $t_{IMU,m+1}$. So navigation results at time $t_{PPS,k}$ is available by applying binomial interpolation [17]. GNSS data at time $t_{PPS,k}$ could be reckoned by the following operation.

$$\begin{cases} x_{SINS}(t_{PPS,k}) = x_{SINS}(t_{IMU,m}) + \dfrac{x_{SINS}(t_{IMU,m+1}) - x_{SINS}(t_{IMU,m})}{t_{IMU,m+1} - t_{IMU,m}}(t_{PPS,k} - t_{IMU,m}) \\[3mm] \Delta x_{SINS} = x_{SINS}(t_{IMU,n}) - x_{SINS}(t_{PPS,k}) \\[2mm] x_{GNSS}(t_{IMU,n}) = x_{GNSS}(t_{PPS,k}) + \Delta x_{SINS} = x_{GNSS}(t_{GNSS,k}) + \Delta x_{SINS} \end{cases} \qquad (18)$$

Initial value of matrix $\hat{X}_0$ and P_0, alongside with the matrix Q and R are set as below.

$$\begin{cases} \hat{X}_0 = \begin{bmatrix} 0.001^\circ & 0.001^\circ & 0.001^\circ & 0\,m/s & 0\,m/s & 0\,m/s & 0^\circ & 0^\circ & 0m \\ & 0.05^\circ/h & 0.05^\circ/h & 0.05^\circ/h & 50\mu g & 50\mu g & 50\mu g \end{bmatrix}^T \\[2mm] P_0 = \mathrm{diag}\big((0.001^\circ)^2,\ (0.001^\circ)^2,\ (0.001^\circ)^2, \\ \qquad (0.01\,m/s)^2,\ (0.01\,m/s)^2,\ (0.01\,m/s)^2,\ (1\,m/R_e)^2,\ (1\,m/R_e)^2,\ (1m)^2, \\ \qquad (0.01^\circ/h)^2,\ (0.01^\circ/h)^2,\ (0.01^\circ/h)^2,\ (10\mu g)^2,\ (10\mu g)^2,\ (10\mu g)^2\big) \\[2mm] Q = \mathrm{diag}\big((0.01^\circ/h)^2,\ (0.01^\circ/h)^2,\ (0.01^\circ/h)^2,\ (10\mu g)^2,\ (10\mu g)^2,\ (10\mu g)^2\big) \\[2mm] R = \mathrm{diag}\big((0.01\,m/s)^2,\ (0.01\,m/s)^2,\ (0.01\,m/s)^2,\ (0.1\,m/R_e)^2,\ (0.1\,m/R_e)^2,\ (0.1m)^2\big) \end{cases} \qquad (19)$$

Comparative experiments of H-infinity Kalman filtering and traditional Kalman filtering under high dynamic environment have been conducted using the simulation system. Comparisons of attitude error, velocity error and position error are shown in Figure 4.

Attitude error mainly caused by colored noise of IMU under high dynamic environment. Comparison of attitude errors indicates that the H-infinity filtering could provide high robustness to some extent. IMU noise and GNSS receiver noise affect velocity and position errors mainly, expecially the up axis results as the height channel of both SINS and GNSS have low precision. Comparison of velocity error and position error indicate that H-infinity filtering has better inhibition of up velocity and altitude error divergency, alongside with a modest improvement at both velocity and position errors.

(a) Attitude error

(b) Velocity error   (c) Position error
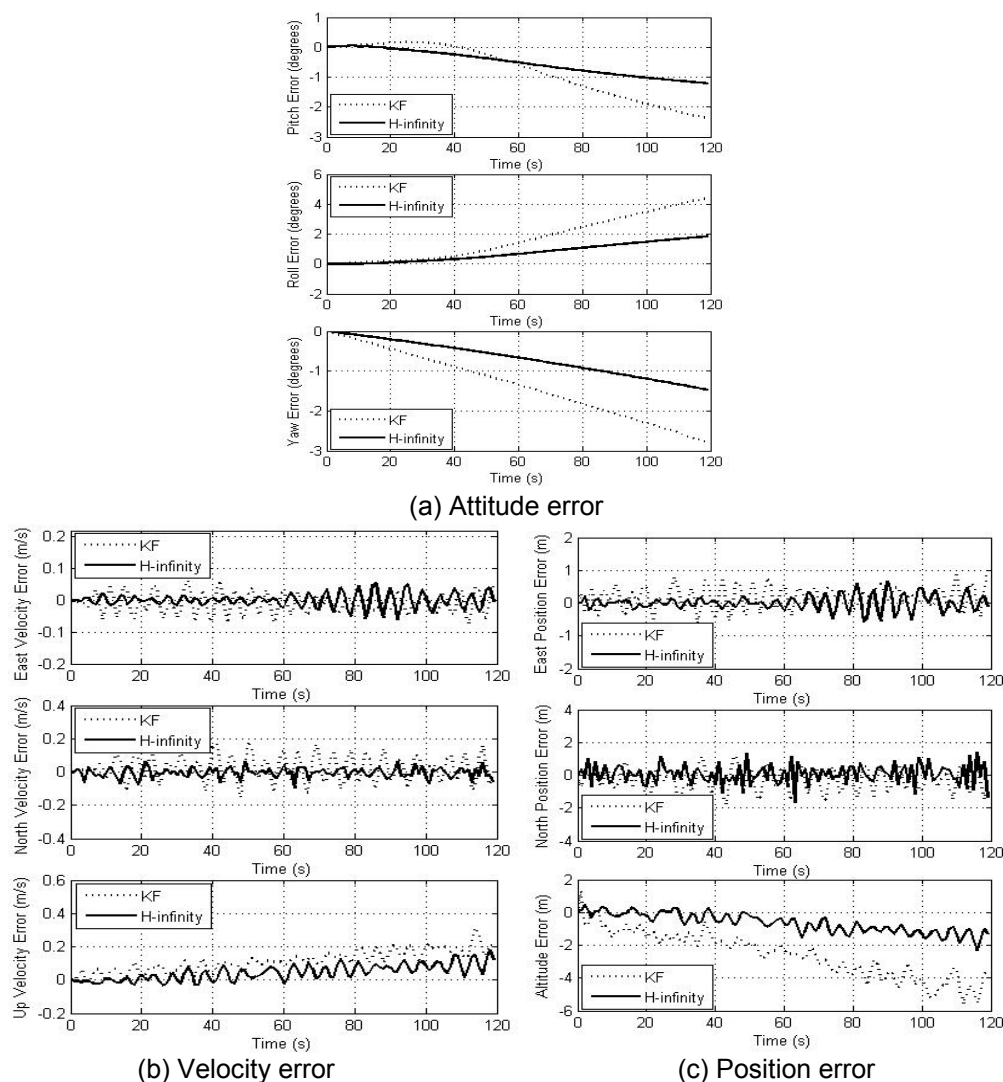
Figure 4. Navigation error comparison

5. Conclusion

This paper presents a kind of H-infinity Kalman filtering algorithm for SINS/GNSS integration method under high dynamic environment. Both designs of the process model and the measurement model are linear, which applys to Kalman filtering or any other linear fusion technologies. A brief design of H-infinity filtering derived from traditional Kalman filtering is used to enhance the robustness performance. Comparative experiments under high dynamic environment based on a hardware-in-the-loop simulation system proved that the H-infinity Kalman filtering has better robustness than traditional Kalman filtering.

References
[1] Titterton DH, Weston JL. *Strapdown Inertial Navigation Technology*. The Institution of Electrical Engineers. 2004.

[2]   Kaplan ED, Hegarty CJ. Understanding GPS: Principles and Applications. *ARTECH HOUSE, INC.* 2006.
[3]   Grewal M, Andrews A. *Kalman Filtering:Theory and Practice Using MATLAB*. Wiley-IEEE Press. 2008.
[4]   Groves PD. Principles of GNSS, Inertial, and Multisensor Integrated Navigation Systems. *ARTECH HOUSE, IN*C. 2008.
[5]   Qi W-J, Heilongjiang U, Zhang P, Nie G-H, Deng Z-L. Robust Weighted Measurement Fusion Kalman Predictors with Uncertain Noise Variances. *TELKOMNIKA Indonesian Journal of Electrical Engineering*. 2014; 12(6); 4692-4704.
[6]   Xie L, Soh YC. Robust Kalman filtering for uncertain systems. *Systems & Control Letters*. 1994; 22(2); 123-129.
[7]   Xie L, Soh YC, De Souza CE. Robust Kalman filtering for uncertain discrete-time systems. *Automatic Control, IEEE Transactions on*. 1994; 39(6); 1310-1314.
[8]   Simon D. Optimal State Estimation: Kalman, H∞, and Nonlinear Approaches. New York: Wiley. 2006.
[9]   Benson DO. A Comparison of Two Approaches to Pure-Inertial and Doppler-Inertial Error Analysis. *Aerospace and Electronic Systems, IEEE Transactions on*. 1975; AES-11(4); 447-455.
[10] Zhou W, Dalian University Of T, Ma H, Wu S, Meng N. INS/GPS Integrated Navigation Technology for Hypersonic UAV. *TELKOMNIKA Indonesian Journal of Electrical Engineering*. 2014; 12(1); 398-405.
[11] Li W, Jia Y. H-infinity filtering for a class of nonlinear discrete-time systems based on unscented transform. *Signal Processing*. 2010; 90(12); 3301-3307.
[12] Lei HR, Chen S, Chang Y, Wang L. Research on the Hardware-in-the-Loop Simulation for High Dynamic SINS/GNSS Integrated Navigation System. *Advanced Materials Research*. 2013; 846-847; 378-382.
[13] Zhao K-R, Xu S, Ye Q, Li Y. *Design and realization of flight simulation system based on Virtual Reality technology*. Control and Decision Conference (CCDC), 2011 Chinese. Mianyang, China. 2011; 4361-4364.
[14] Niu X, Yan K, Zhang T, Zhang Q, Zhang H, Liu J. Quality evaluation of the pulse per second (PPS) signals from commercial GNSS receivers. *GPS Solutions*. 2014; 1-10.
[15] Li G, Mu J, Xu H. Measurement study for accelerometer based on injection current. *Journal of Astronautic Metrology and Measurement*. 2000; 20; 6-7.
[16] Xie W, Cai Y, Yao J, Xin C. *Design and implementation of the LIMU pulse counting system*. IET Conference Proceedings. Xiamen, China. 2012; 778-781.
[17] Zhang P, Gu J, Milios EE, Huynh P. *Navigation with IMU/GPS/digital compass with unscented Kalman filter*. Mechatronics and Automation, IEEE International Conference. Niagara Falls, Ont., Canada. 2005; 3; 1497-1502.